9

# Controlling and Simulation of Stray Currents in DC Railway by Considering the Effects of Collection Mats

Mohammad Ali Sandidzadeh and Amin Shafipour
*School of Railway Engineering, Iran University of Science and Technology, Tehran, Iran*

## 1. Introduction

Urban rail transit systems are mostly electrically DC type. Usually in these systems for reducing the costs, running rails are used as the return current paths. Because of the electrical resistance of rails against the flow of traction currents and also rail to ground conductivity (despite rail-to-ground insulations), parts of the return current that flow from trains to traction substations leak to the ground. These leaking currents are called stray currents (as shown in Fig. 1). Stray currents can enter their neighboring metallic infrastructures and, as a result of anodic interactions, cause electrochemical corrosions in their leakage path.

The amount of electrochemical mass reduction as a result of anodic interaction due to flow of current *i(t)* from a metal to an electrolytic environment can be gained as below

$$M = C\int_{t1}^{t2} i(t)d(t) \tag{1}$$

in which *C* is the electrochemical coefficient and is based on the type of the metal, electrolyte, and chemical calculations. For example, *C* is 9.11 $KgA^{-1}Year^{-1}$ for iron. It means that a current of 1 ampere can oxidize 9.11 kilograms of iron per year. This can reduce the safety and the life time of structures and infrastructures in tunnels. The corrosions caused by stray currents yield a total loss of $500 million each year to the American railway system [1]. When a train is running, especially during its accelerating time, the traction supply current can sometimes reach 6000 amperes. Since the resistance of rails is between 15 to 20 $m\Omega Km^{-1}$, the return current can face a voltage drop of up to 120 $VKm^{-1}$. This voltage, due to inadequate insulations of rails and their underlying structures, allows the current to leak to the ground. Stray current control is usually done via improvements performed to transportation systems or the neighboring ground structures. Increasing the resistance between rail and ground is a very effective method in reducing stray currents. The increase in resistance reduces the tendency of return current to flow in any path other than the rails. Other methods for avoiding corrosions include cathodic protection, rail insulation, traction voltage increase, employment of proper rails that have very low electrical resistance and usage of proper grounding systems in traction substations.

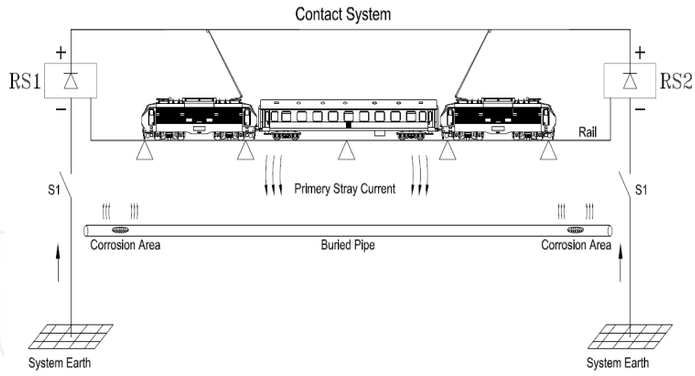


Fig. 1. Exposure of Stray Current in DC Railway Systems.

Despite application of the mentioned methods for controlling stray currents, some portion of the traction current would still flow through the ground instead of the rails to reach the negative terminal of the substation. In this paper, by discussing the ways for using stray current collection mat and grounding system via simulations, the effects of collector cables and stray current collection mats below the rails are described.

Many papers, published between 1995 and 2005, discussed and examined various grounding systems in railway transportation. In addition, general techniques for reducing voltage and stray current levels were discussed in these papers. "Paul" specifically examined grounding in power grid systems of subways [2]. "Goodman", for the first time, calculated the rail voltage and stray current profiles. His calculations were not computer aided and instead based on simple hypothesis [3]. Later, "Case" used Π model to investigate a diode grounding system and compared it with EN50122-2 standard [4]. "Lee" used the floating models instead of "Case"'s proposed Π model [5, 6]. Although Lee's model benefited from high accuracy, it showed no significant different results. In the mentioned papers, the effects of grounding systems on voltage and stray current profiles were investigated. Despite mentioning corrosion in the previous papers, it was "Cotton" who, for the first time, discussed the influence of soil structures and stray current collection mats on corrosion performance of metallic infrastructures. The outcome of his survey was software that analyzed and studied influences of soil and current collection mats on corrosion of metallic infrastructures [7].

"Cotton" discussed the importance of stray current reduction in DC rail transit systems and proposed usage of stray current collection mats. Also, he talked about the influences of his proposed system's performance and resistivity of soil on stray currents and the resulting corrosions [8].

"Lee" used the floating model to simulate and investigate stray currents and their effects on underground structures. He used a coefficient of 0.1V voltage increase of these structures as a high stray current leakage in these systems. In the end, he proposed some methods for reducing stray currents by improving railway systems and the neighboring structures [9].

In this research, after a brief introduction of Tehran Metro line 4, the present methods used for simulation and analysis of stray currents are investigated and later stray current and touch potentials are studied by simulating the current path between two substations of line

4. The simulations are performed for various grounding scenarios of traction substations and the influence of stray current collection mats, under various scenarios, and effective parameters on performance improvement of the collection system, in the simulated line, are discussed. In the end the stray current and touch potential of rails under presence and absence of the stray current collection mats, in the worst scenarios, and movement of four trains from three stations, with the middle station not having a traction substation, are investigated.

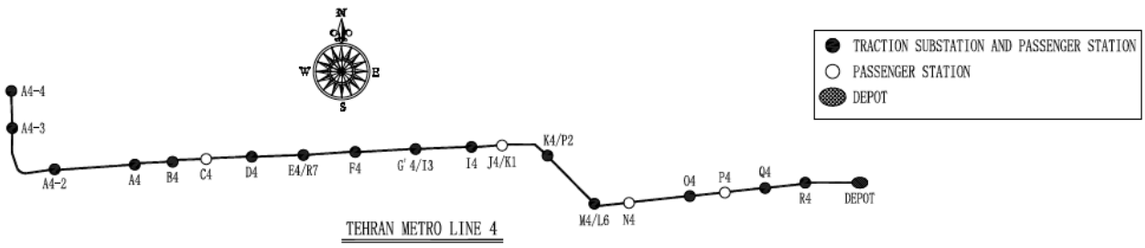


Fig. 2. Tehran Metro line 4 plan

## 2. An introduvtion of Tehran metro line 4

Tehran metro line 4 is the forth subway line in Tehran with a length of 25 Km and comprises 22 stations. It is stretched from the west to the east part of the city and is equipped with 18 traction substations. The details of the substations are shown in tables 1 and 2. The total trip time in line 4 is 42 minutes, which includes 25 seconds of dwell time in each station. At the most crowded hours, the train headways reach 2 minute cycles. Fig. 2 shows the line 4 plan.

Each traction substation is supplied with two rectifier transformers that have nominal powers of 2.5 or 3.3 MW. The required power is supplied directly by 63 KV power grid of Tehran Regional Electric Co. in B4, H4 and R4 substations, and is then stepped down to 20 kV via 3×2 (63 to 20kV) transformers (Fig. 3). After that, it is distributed in LPSs (Lighting and Power Substations) and RSs (Rectifier Substations) by means of separate 20 kV rings.

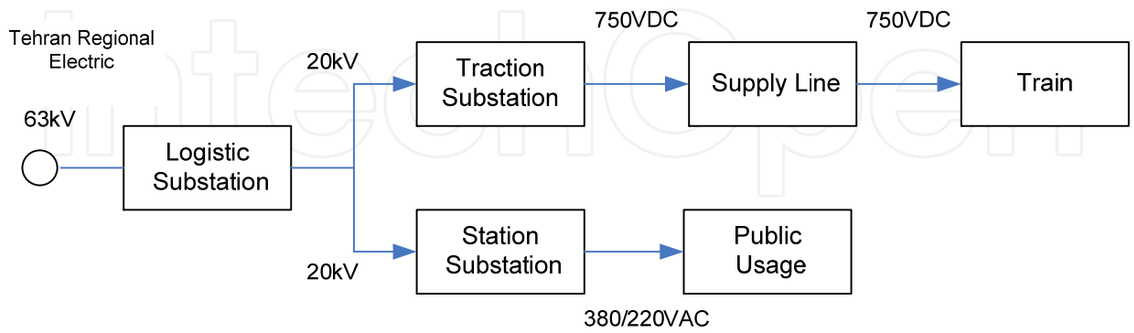


Fig. 3. General diagram of Tehran Metro Line 4 power system.

For a 750V power supply, under full load and setting of 6%, the substation output voltage has a voltage drop of 45V. Since the train requires high power amounts during its acceleration, the RS should be able to supply the extra required load. Based on class VI in

compliance with IEC146 standard, the RS should be capable of a constant load supply of 100%, a nominal load supply of 150% for a period of 2 hours and a nominal load supply of 300% for a period of 1 minute. Based on its internal resistance, at 300% overload times, the voltage drop in the RS would be around 135V.

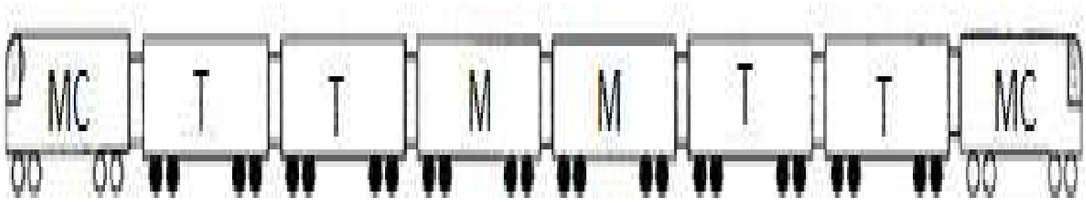


Fig. 4. The order of rolling stock cars

The trains comprise 8 cars and weigh around 274 tons without passengers and 379 tons in normal transit conditions (Fig. 4). The traction power is supplied from 750V voltage source and from the third rail. Each train includes 16×200kW traction motors. The maximum train speed and acceleration is 80 $kmh^{-1}$ and 0.2 $ms^{-2}$, respectively. The rolling resistance equation (i.e., the Davis formula) is $1.57+0.00106V^2$ for the traction mode and $1.97+0.0025V + 0.00106V^2$ for the breaking mode. Also, the internal auxiliary power consumption of each train is 125 kW.

| Item | Station Name | Station Characteristics | | |
|---|---|---|---|---|
| | | Begin | Center | End |
| 1 | A4-6 | | | |
| 2 | A4-5 | -3+645 | -3+566 | -3+487 |
| 3 | A4-4 | -1+611 | -1+532 | -1+453 |
| 4 | A4-3 | -0+15 | 0+063 | 0+142 |
| 5 | A4-2 | 1+661 | 1+740 | 1+819 |
| 6 | A4 | 2+811 | 2+890 | 2+969 |
| 7 | B4 | 3+971 | 4+050 | 4+129 |
| 8 | C4 | 4+926 | 5+005 | 5+084 |
| 9 | D4-H2 | 5+645 | 5+724 | 5+803 |
| 10 | E4 | 7+064 | 7+143 | 7+222 |
| 11 | F4 | 8+153 | 8+232 | 8+311 |
| 12 | I3G'4 | 9+427 | 9+506 | 9+585 |
| 13 | I4 | 10+716 | 10+795 | 10+874 |
| 14 | K1J4 | 11+310 | 11+389 | 11+468 |
| 15 | P2K4 | 12+461 | 12+540 | 12+619 |
| 16 | M4 | 13+773 | 13+852 | 13+931 |
| 17 | N4 | 14+537 | 14+616 | 14+695 |
| 18 | O4 | 15+593 | 15+671 | 15+750 |
| 19 | P4 | 16+489 | 16+568 | 16+647 |
| 20 | Q4 | 17+443 | 17+522 | 17+601 |
| 21 | R4 | 18+793 | 18+872 | 18+951 |
| 22 | S4 | 20+661 | 20+740 | 20+819 |

Table 1. Characteristics of line 4 stations

| Item | Station Name | Type of Substation | Capacity |
|---|---|---|---|
| 1 | A4-6 | RS | |
| 2 | A4-5 | RS | 2×3300 |
| 3 | A4-4 | RS | 2×2500 |
| 4 | A4-3 | RS | 2×3300 |
| 5 | A4-2 | RS | 2×2500 |
| 6 | A4 | RS | 2×2500 |
| 7 | B4 | RS | 2×2500 |
| 8 | C4 | RIC | - |
| 9 | D4-H2 | RS | 2×2500 |
| 10 | E4 | RS | 2×2500 |
| 11 | F4 | RS | 2×2500 |
| 12 | I3G'4 | RS | 2×2500 |
| 13 | I4 | RS | 2×3300 |
| 14 | K1J4 | RIC | - |
| 15 | P2K4 | RS | 2×3300 |
| 16 | M4 | RS | 2×3300 |
| 17 | N4 | RIC | - |
| 18 | O4 | RS | 2×3300 |
| 19 | P4 | RIC | - |
| 20 | Q4 | RS | 2×3300 |
| 21 | R4 | RS | 2×2500 |
| 22 | S4 | RS | 2×3300 |

Table 2. Characteristics of line 4 substations and their capacities

## 3. Stray current modeling

For simulation of a DC traction network and analysis of stray currents, two different methods can be used. The first method is based on the floating model and distributed elements [5, 6]. In this method, distributed elements like rail conductance and resistance per unit length are used for the calculations, and by utilizing the floating equations, the equations for stray current and touch voltages of rails are determined. Equations (2) and (3) show the current and voltage in various parts of the rail, respectively as below: [6]

$$i(x) = c_1 \exp(\gamma x) + c_2 \exp(-\gamma x) \tag{2}$$

$$v(x) = -R_0(c_1 \exp(\gamma x) + c_2 \exp(-\gamma x)) \tag{3}$$

in which $i(x)$ is the rail current, $v(x)$ is the rail voltage, $\gamma$ is the propagation constant ($=\sqrt{RG}$), $R_0$ is the characteristic resistance of the rail ($=\sqrt{R/G}$), $c_1$ and $c_2$ are the equitation constants and determined based on the boundary values, $R$ is the resistance per unit length of the rail and $G$ is the leakage conductance between the rail and the ground. Although this method has the ability of determining quantities in each part with high accuracy, it has a low flexibility and therefore for various structures, many of its equations should be altered.

The second method is based on using concentrated elements or Π line model in the DC mode. In this method, the line is divided into sections with equal lengths and each section is modeled with a rail to ground resistance and conductance (Fig. 5). In most applications, selecting the length of each section as 100 meter creates a good accuracy for stray current determination. Each substation is modeled via its Thevenin equivalent (i.e., a voltage source and an equivalent resistance) or Norton equivalent circuit. The train is also modeled via a time-varying current source. Finally, based on proposed model and node analysis rules, rail surface potential and the current amount profiles are resolved. The linear equation for node analysis is as below: [4]

$$\overline{Y}_n \cdot \overline{e} = \overline{i}_s \tag{4}$$

in which $\overline{Y}_n$ is the node admittance matrix, $\overline{e}$ is the node voltage matrix and $\overline{i}_s$ is the node current sources matrix. In the node admittance matrix, $y_{ii}$ entry is the sum of all conductances tied to the *i*th node and $y_{ij}$ is the negative of the sum of all conductances between the *i*th and the *j*th nodes. Also, $i_{si}$ is the sum of all currents entering the *i*th node. The currents entering the positive and exiting the negative nodes are also considered here. The node voltage matrix is the unknown matrix that is determined by solving the above equation. This matrix actually represents the amount of rail surface voltage.

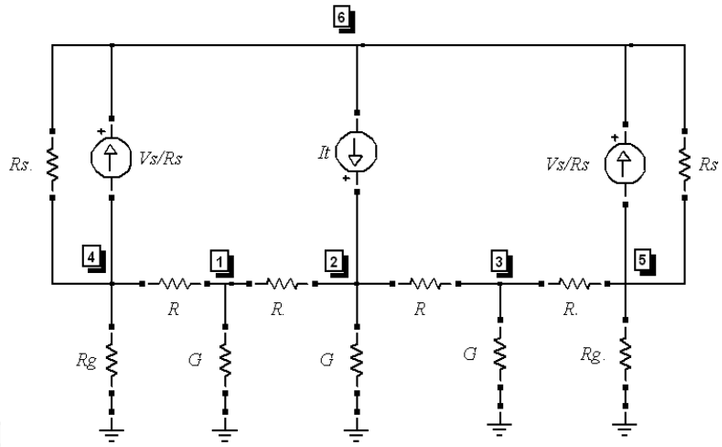


Fig. 5. Simplest form of discrete Norton line model for two stations and rail

Because of the existence of resistance network, the admittance matrix is symmetrical and has a positive determinant. The voltage of the station rectifier can be determined from the DC load distribution of the traction network. The current amount in the $I_T$ current model, which is the train model, can be determined from the train's current – velocity equations.

Fig. 6 shows the calculation steps based on this model in a DC railway network. According to the presented flowchart, at first, based on the train time schedule, the locations of various trains are determined and then each substation voltage is gained by distributing the load through the system. Also, the traction current of each train is determined according to the velocity of that specific train. Finally, by solving the node equations, the touch voltage and stray current for each node are calculated. [10]

Although this method is not as accurate as the first one, selection of 100-meter sections creates the acceptable preciseness required for analysis of stray currents. Besides, this method allows simulating and modeling different structures with minimal changes in them. Since all the equations in this method are linear, the simulations have an acceptable performance.

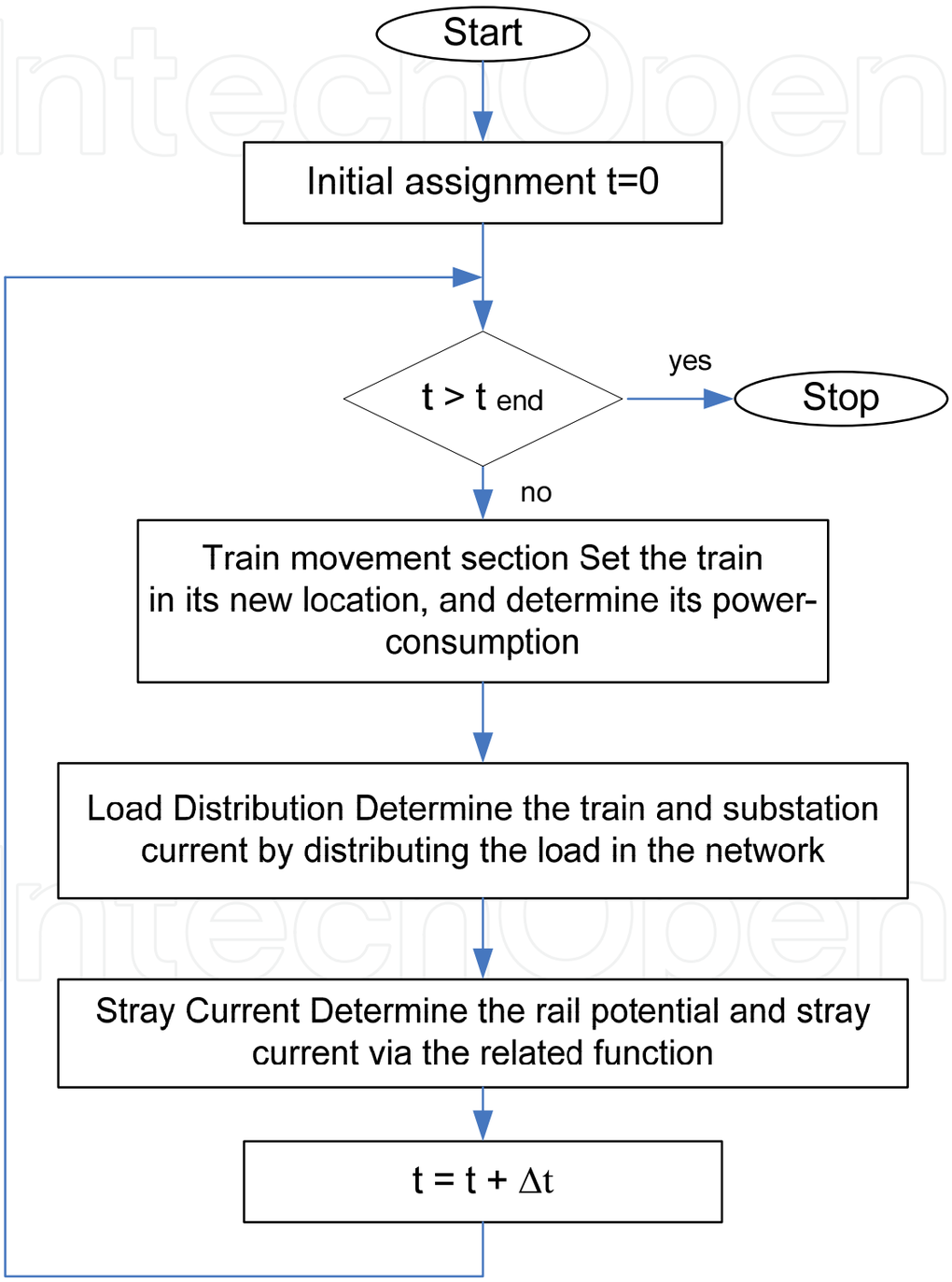


Fig. 6. Flowchart for determining the touch potential and stray current in the discrete model

## 4. Modeling the line and determining the parameters

For line modeling, Fig. 7 schematic is used, in which $V_{dc}$ is voltage of the DC busbar, $I_t$ is the train model, $R_{rr}$ is the resistance per unit length of the rail, $R_{rm}$ is the rail to mat resistance, $R_{mm}$ is the resistance per unit length of the mat and $R_{mg}$ is the mat to ground resistance. Also, $R_g$ is the resistance of the substation ground. The type of grounding can be defined based on the way the negative substation busbar is connected to the ground; if, as shown in Fig. 7, $S_1$ key is closed, the system is grounded and if this key is open, the system is floating. If a diode is used instead of $S_1$ key, then the system is diode grounded.

The amount of $I_t$ current varies based on the train velocity and is calculated from the power consumption of traction motors and the Davis formula. Fig. 8 shows the relation between the current and speed of the traction motors.

The parameters used in the simulation are determined from the available line 4 characteristic data, the available standards, references [8], [11] and division of the line into equal 100 meter cells. According to the manufacturers' data, $R_{rr}$ is 1650 μΩ (i.e., with 5% corrosion, the resistance per unit length of the rail is 16.5 $\mu\Omega m^{-1}$.) The rail to soil conductivity, based on the type of foundation, is 10 $\Omega km^{-1}$ and therefore $R_{rm}$ is assumed to be 100Ω. Assuming the special resistance of steel as 15.9 $\mu\Omega cm^{-1}$, a corrosion coefficient of 5% and a cross sectional area of 1800$mm^2$ for the underground stray current collection mat, the amount of $R_{mm}$ is calculated as 12mΩ. The stray current collector cable with a cross sectional area of 185$mm^2$ is assumed to have a resistance per unit length of 180 $\mu\Omega m^{-1}$. The $R_{mg}$ is assumed to be 1Ω.

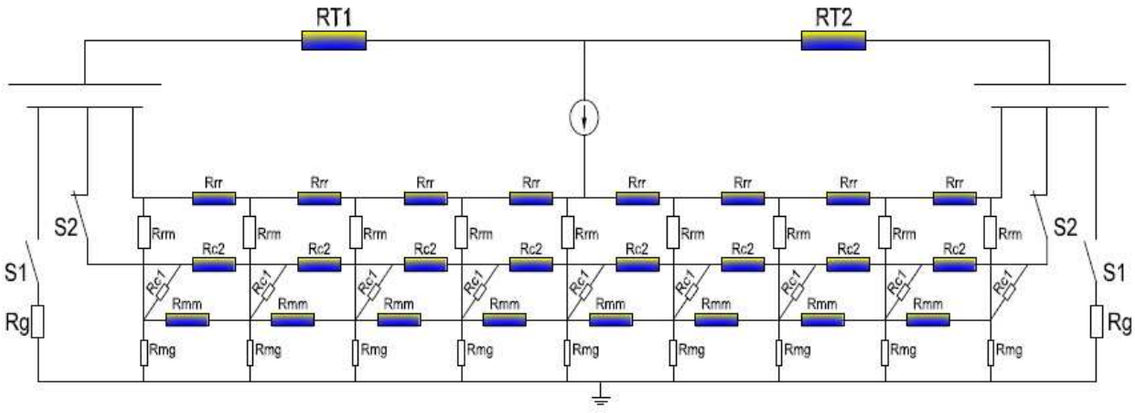


Fig. 7. The schematic used for line modeling

Since the grounds in I3G4 and F4 stations have the lowest resistance values, the line between the two stations, which is 1274 meters long, is selected for the simulation. Fig. 9 shows the time-speed relation for this line.

As shown here, the train starts its movement with acceleration of 0.75 $ms^{-2}$ and after 330 meters reaches a speed of 80$kmh^{-1}$. Then the supply from the power source is cut and the train runs the rest of the line as the result of its inertia, and its speed starts to decrease. After 1150 meters the dynamic brakes are engaged and the train begins to stop.

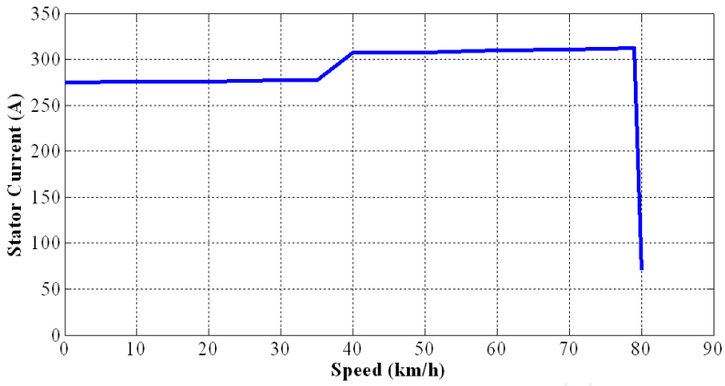


Fig. 8. The current-speed relation of train traction motors in the power consumption and return modes

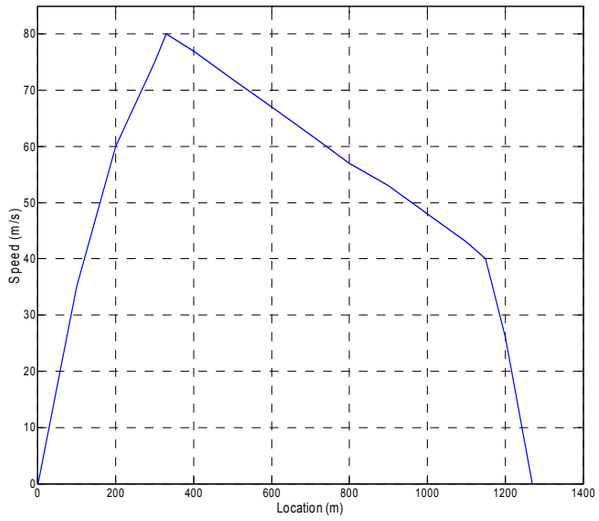


Fig. 9. The train speed-location curve

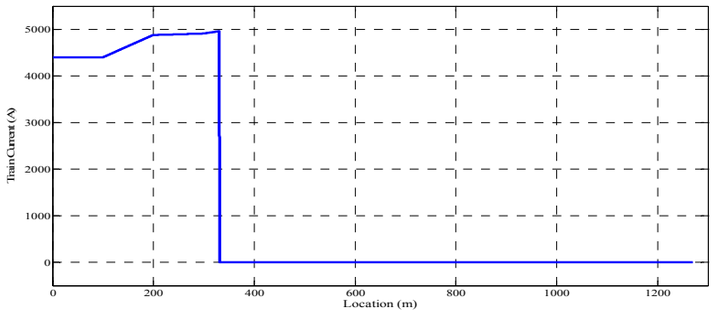


Fig. 10. Current – location curve of traction motor

Fig. 10 shows the current-speed curve in the line. It shows the total train consumed current for all the 16 traction motors. Since stray current effect on metallic structure in long term, in this analysis transition currents and the current related to train auxiliary power have been ignored. Also, the train regenerative current is lossed on the resistors located on the train.

## 5. Simulation results and analysis

For analyzing level of the stray current for Tehran Metro line 4, the simulations are performed under various scenarios. In the first scenario, while no collection system is utilized, effect of grounding systems on current leakage from rail is studied; then in the second scenario while the reinforcement grid exit in the second stage of concrete under rail, effect of electrical continuity of this grid on controlling and collecting stray current is investigated. In the next scenario, stray current collector cable is added to collection mat and in the last part, previous scenarios are considered on the passenger stations (without traction substations).

### 5.1. Effect of grounding systems

This part is when no stray current collection system is utilized and train is assumed to be running and 2 below cases are studied:

At first, while the train is in a specific location, the stray current and rail potential is observed along the whole line (case I) later, the stray current is studied for a specific location, while the train moves along the whole line (case 2) finally, the effects of the collection mats and then the collector cable, in addition to the mats, are investigated.

#### 5.1.1 Case I

The first mode is when the train is at a location 100m from the start substation and is accelerating, while a current of 4400 amperes is fed to the train via the third rail. Such that, a current of 4060 amperes is fed to the train from the nearest substation. Fig. 11 shows the leakage current from rail and fig.12 shows potential of running rail along the way for three different grounding systems.

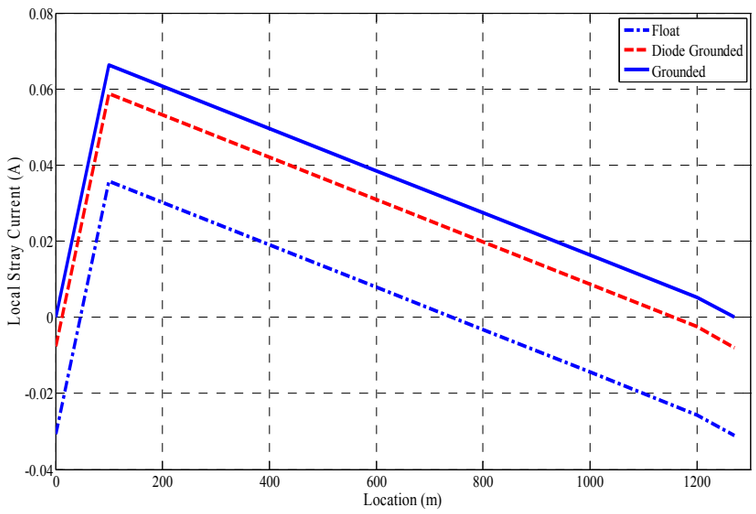


Fig. 11. Leakage current from rail for three different grounding system when the train is 100 meters away from the initial substation

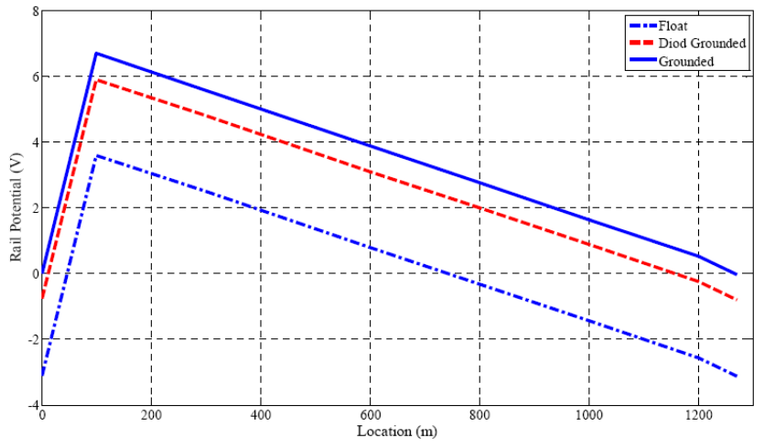


Fig. 12. The rail touch potential for three different grounding systems when the train is 100 meters away from the initial substation

It can be concluded from the presented graphs that in all three grounding system, the current is leaking from the rail to the ground in locations where rail to ground voltage is positive, and the amount of current flow depends on the rail voltage with respect to ground. In solidly grounded systems, due to the zero voltage at the substation and the positive rail to ground voltage, stray current leakage is observed in all locations of the line. In diode grounded system less stray current leakage is observed, since the rail voltage is negative at the substation. The reason for this is that diodes turn on only when the voltage of their cathode is -0.8v less than their anode voltage. In ungrounded system, the stray currents case is much improved. In the first half of the line, from the train to the substation, stray currents leak and flow from the rail to the ground (since the rail to ground voltage is positive,) and in the second half of the line, the leaked stray current flow back to the rail. The cumulative stray current in the floating system is 0.136 amperes, while it is 0.33 amperes in the diode grounded and 0.42 amperes in direct grounded systems.

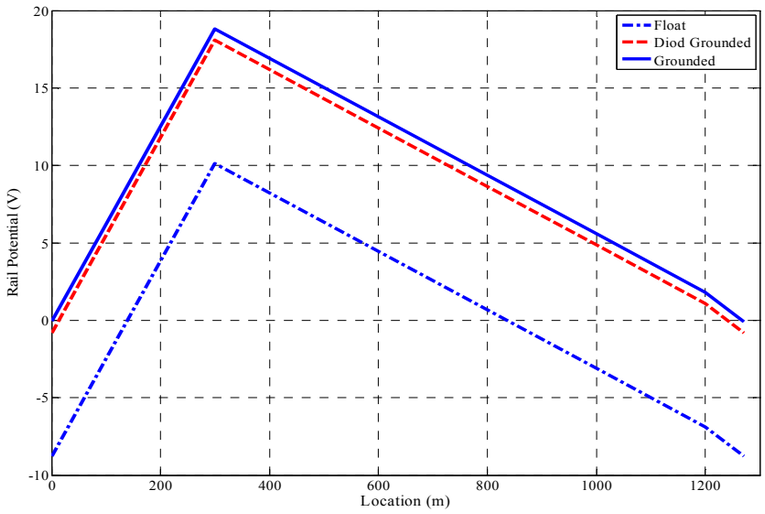


Fig. 13. The rail touch potential in three different grounding systems when the train is 300 meters away from the initial substation

When the train is 300 meters away from the initial substation, its current amount reaches a maximum of 4960 amperes. From this current, 3814 amperes are supplied by the first and 1146 amperes are supplied by the second substation. Because of the increase in traction current in this case, the stray current and touch potential are also amplified for the three grounding systems (Fig. 13 -14). As it is shown, touch potential in grounded system in nearly zero in substations and it's positive in other locations. Also it's approximately twice that of the floating system in train location. In this case, the amount of rails stray current increases to 1.1 amperes in the grounded system, 1.0 amperes in the diode grounded system and 0.3 amperes in the floating system.

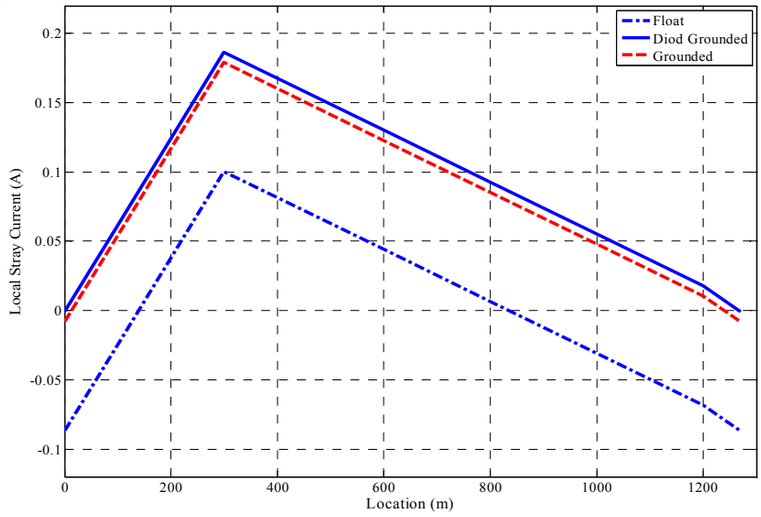


Fig. 14. Leakage current from rail for the three different grounding systems when the train is 300 meters away from the initial station

### 5.1.2 Case II

At first the investigation is done for a location that is 100m away from the initial first substation. Fig. 15 presents the resulting stray current for the grounding systems. As shown, the floating system has the lowest amount of stray current among all the existing grounding systems, and when the train is more than 200 meters away from the initial substation, current return from the ground to the rail is also observed. In the grounded system of Fig. 15, at all points of the rail, current leakage, which is more than the other systems, is observed. The highest amount of stray current is observed when the train is near the 100 meter point.

In solidly and diode grounded systems, in which the rail voltage about the substation is zero, even after the train has passed location 100m, the rail voltage near the substation remains positive and the current leakage continues, although at lower magnitudes. The traction current, however, increases up to location 330 m. In the floating system when the train passed location 200m, the rail voltage at location 100m point become zero and the flow of stray current stops. However, further train running makes the voltage of this location negative and therefore the stray current flows back to the rail.

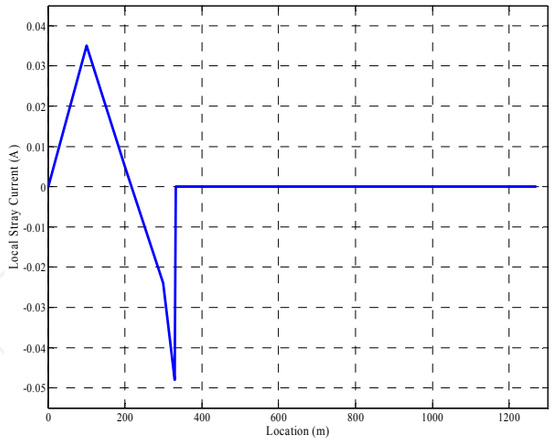


(a)

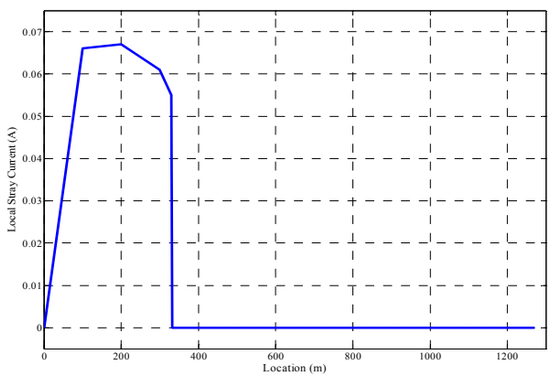


(b)

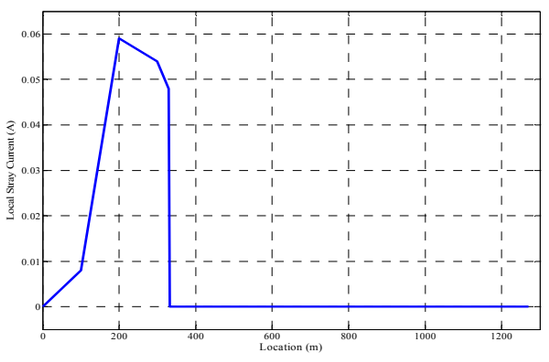


(c)

Fig. 15. Stray current at location 100 m on the rail in case II for a) The floating system b) Solidly grounded system c) Diode grounded system

Fig. 16 shows the stray current at location 300 m in the line. Like the previous instances, the stray current is at its peak when the train is also at this location. At location 300m, due to sufficient distance from the substation, unlike location 100 m, always in all grounding system, when there is current flow, the touch potential is positive and stray current exists.

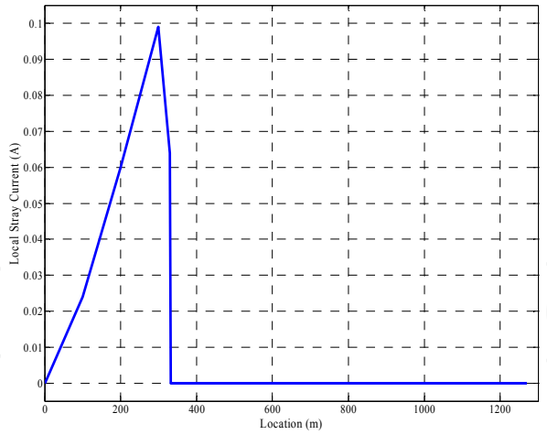


(a)

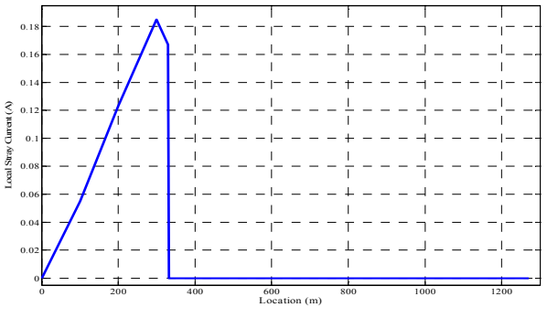


(b)

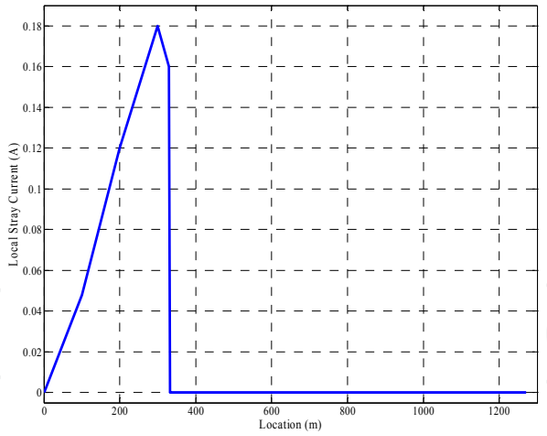


(c )

Fig. 16. The stray current at position 300 m, on the rail in case II for A) Floating system b) solidly grounded system c) Diode grounded system

Fig.17 shows the stray current at location 1000 m from the initial substation. The voltage at this location is just similar to the voltage at location 100 m, however the stray current is lower and the current amount that returns from the rail to this point is higher. In the floating system, since this location is closer to the first substation, its voltage remains negative and the current keeps flowing back to the rail.

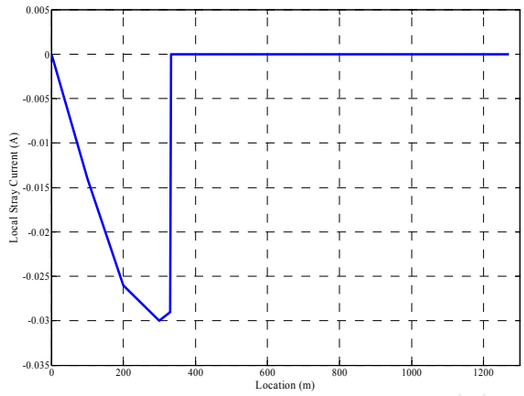


(a)

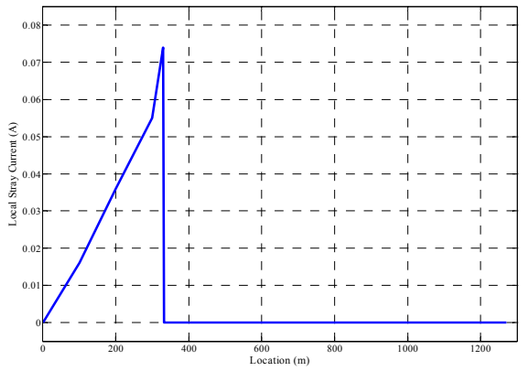


(b)

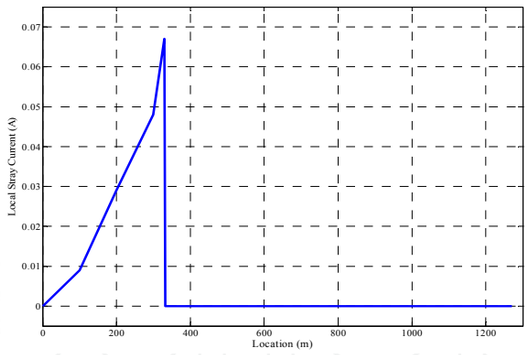


(c)

Fig. 17. Stray current at location 1000 m when the train is running for a) Floating system b) Solidly grounded c) Diode grounded system

### 5.2 Using stray current collection mat

The simulations in this section are performed assuming the presence of a reinforcement bars. If the metal bars in the concrete under the rail intersect with each other, they collect main portions of stray currents due to creating a low resistance path for conducting these currents from rail to traction substation. So this collection mat result increasing leakage current from rail because of making return path to traction substation. Some portions of

stray currents leak from the rail to metal bars of the reinforced concrete and continue to flow through the underlying concrete structure. If this current is not returned to the substation through a specific current path, the current leak from the concrete structure to the ground would create corrosions in the metal bars of the concrete. In fact for executing reasons, the mats are installed in sections with length of 100 m such that there is a gap of nearly 100 mm between sections. If there is no electrical connections (by wire or cable) between separate sections of mat, entering current to this structure cause severe damages to them.

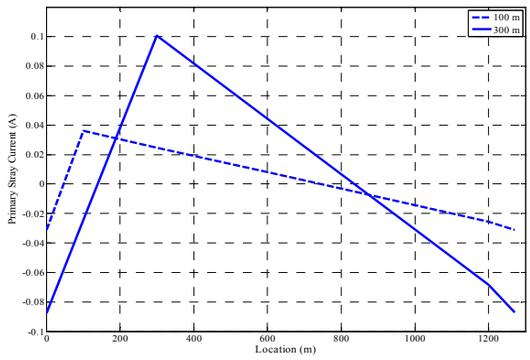


(a)

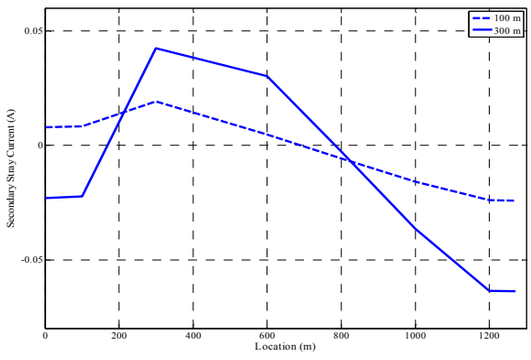


(b)

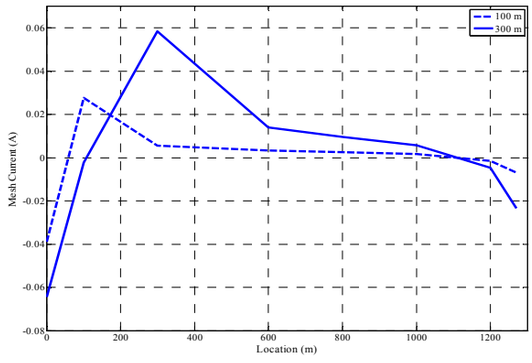


(c)

Fig. 18. Stray current when the train is at locations 100 m and 300 m from the initial station and the metallic concrete structure is unprotected a) Stray current leak from the rail b) Stray current leak to the ground c) Current entering the concrete collection mat

In the first part, this metallic structure is consumed disconnected and there is no direct return path to substation for current that enters which results are shown is fig. 18.

In this case, in the floating system, stray current leak from the rail when the train is at location 100m from the first substation is 1.37 amperes, of which 0.06 amperes flows through the concrete's metallic structure and causes severe damages to this structure. When the train is at location 300m, the stray current becomes 0.3 amperes, of which 0.145 amperes flows through the collection mat. Also about 50% of stray current from rail doesn't enter to this mat. To overcome this flaw, in addition to interconnecting all parts of the mat to each other, a path for connecting the collection mat to the negative busbar of the substation should be provided. This connection is done by means of a diode that helps having cathodic protection and making the current flow one directional (Fig. 19).

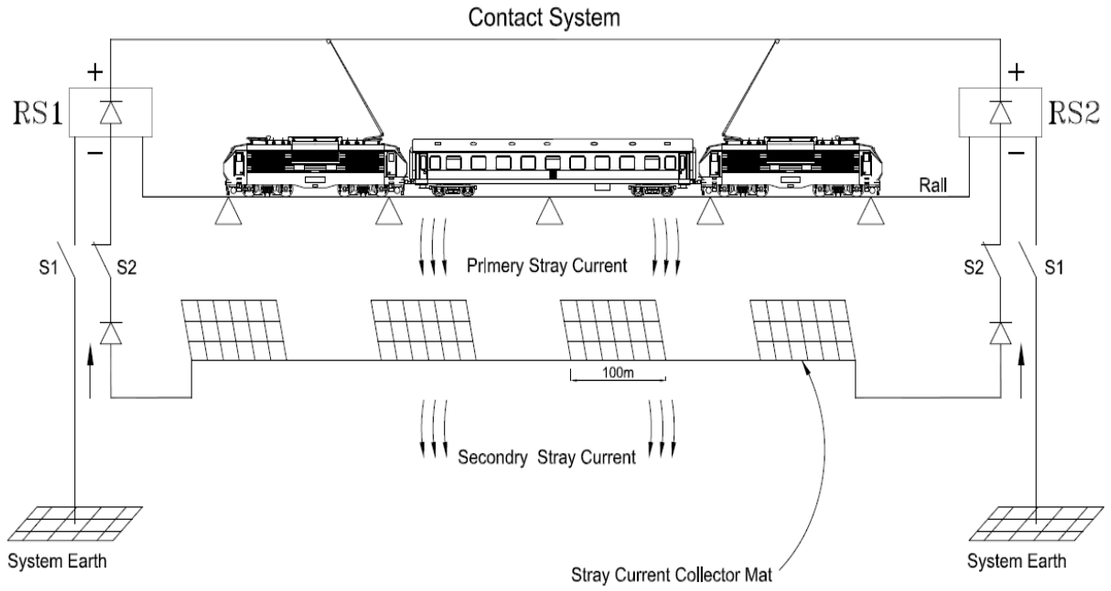


Fig. 19. Using the concrete metallic structure as the stray current collection mat

Fig. 20 shows the stray current from rail when the train is at locations 100m and 300m from the first substation and the stray current collection mat is used. Because of the mat to ground resistance and connection of the mat to the negative busbar by the diode, the situation here is like that of the diode grounded system. In this case, although the substation ground is considered floating, the substation voltage remains around zero (which is the diode on voltage) and the rail touch potential at the train's location becomes more than the floating system's voltage and, as a result, the stray current increases. Fig.21 shows the current which captured by the collection mat and as shown this amount has increased compared to previous part. However, as shown in Fig. 22, a large portion of the stray current is collected by the collection mat and only a small portion of it leaks to the ground. In this case, the total rail output current at locations 100m and 300m are 0.33 and 1.01 amperes, respectively, of which 0.065 and 0.099 amperes leak to the ground, respectively, and the rest is collected by the mats. Using equation (5) for evaluating the efficiency of the stray current collection system, the system performance becomes 81% at position 100m and 90% at position 300m.

The equation is

$$\eta = (I_{Collected} / I_{st}) \times 100 \tag{5}$$

in which $I_{Collected}$ is the amount of stray current collected by the mats and $I_{st}$ is the total stray current that has leaked from the rail. As shown in Fig. 22, the highest amount of stray current leakage occurs in the middle point of the line. The reason for this is the long distance of this position from the substations. Although the highest stray current is observed at location 300m, the stray current at location 600m is also high and is 70% of the stray current amount at location 300m. Besides, since location 600m has the highest distance from the line terminating substations, the resistance remains high at this location for stray currents that enter the mats, and this makes this middle position to have the highest rate of stray current leakage to ground in the entire line.

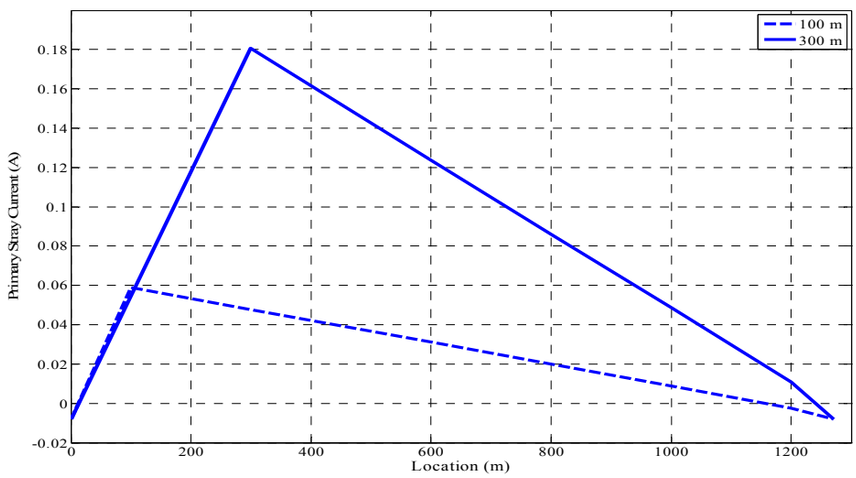


Fig. 20. Rail stray current when the train is at locations 100 m and 300 m and collection mats are used

In Fig. 23, the efficiency of the collection system, based on changes of the cross sectional area of the mat is presented. As mentioned before, the mats used in Tehran Metro line 4 have cross sectional areas of 1800 mm². The higher the cross sectional area of the mat, the lower its resistance per unit length and the higher its stray current collection amount would be. $R_{mm}$ is 27.4 mΩ for a cross sectional area of 700 mm² and 8 mΩ for a cross sectional area of 2400mm². Fig. 23 shows the graph for the time the highest traction current supply, when the train is at position 300 m.

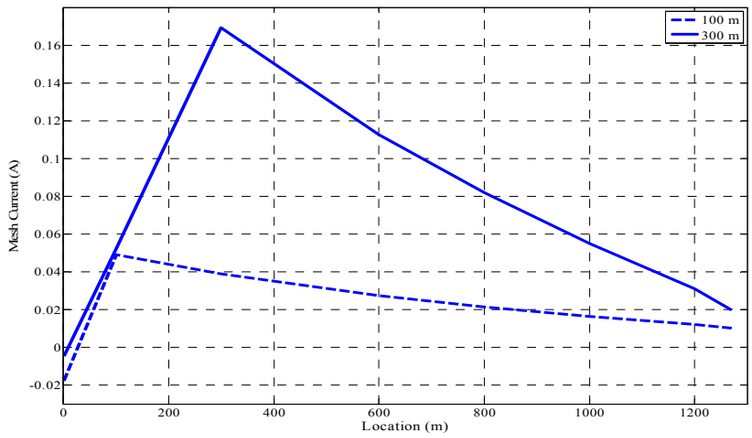


Fig. 21. The current collected by the mat when the train is at locations 100 m and 300 m from the initial substation and stray current collection mat is also used

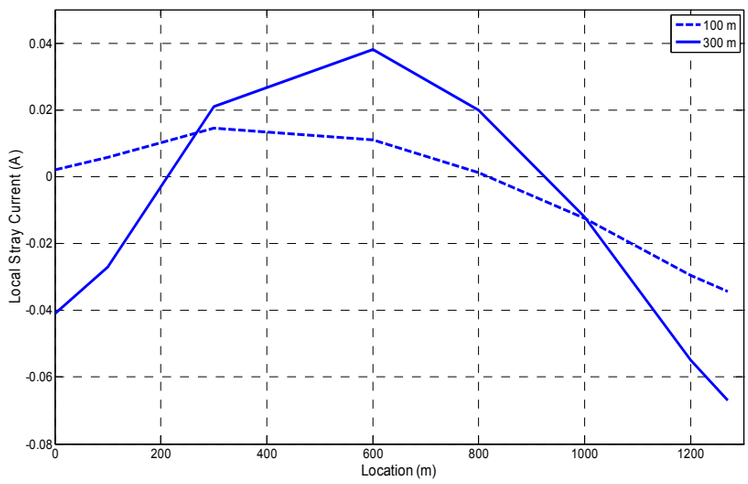


Fig. 22. Stray current leakage to ground when the train is at locations 100 m and 300 m from the first substation and collection mat is used

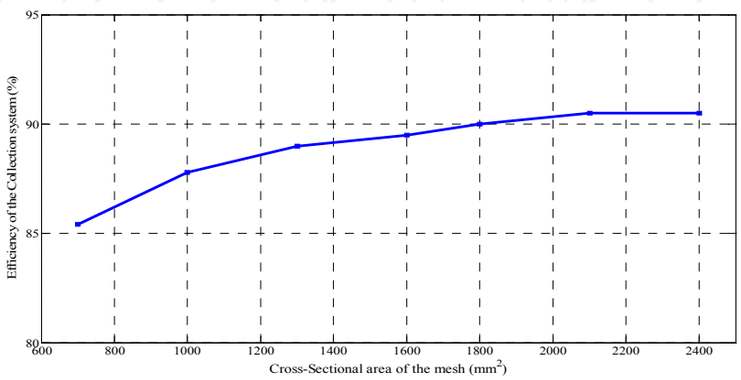


Fig. 23. Efficiency of Stray current collection system based on changes of the cross sectional area of the mat at location 300 m (the worst scenario)

### 5.3 Using stray current collector cable

Due to the problems in building a continuous collection mat system, existence of current in the mat system increases the chance for stray current leakage from the mat system itself (especially at connection points). For protecting and retaining high efficiency of the mat system, stray current collector cables are used. Stray current collector cables are installed alongside the rail and they are, at specific locations (e.g., connection points,) connected to the underlying stray current collection mat. In this way these cables provide a low resistance and insulated parallel current path that canalizes and directs the main part of the mat currents to the negative busbar of the substation (Fig. 24).

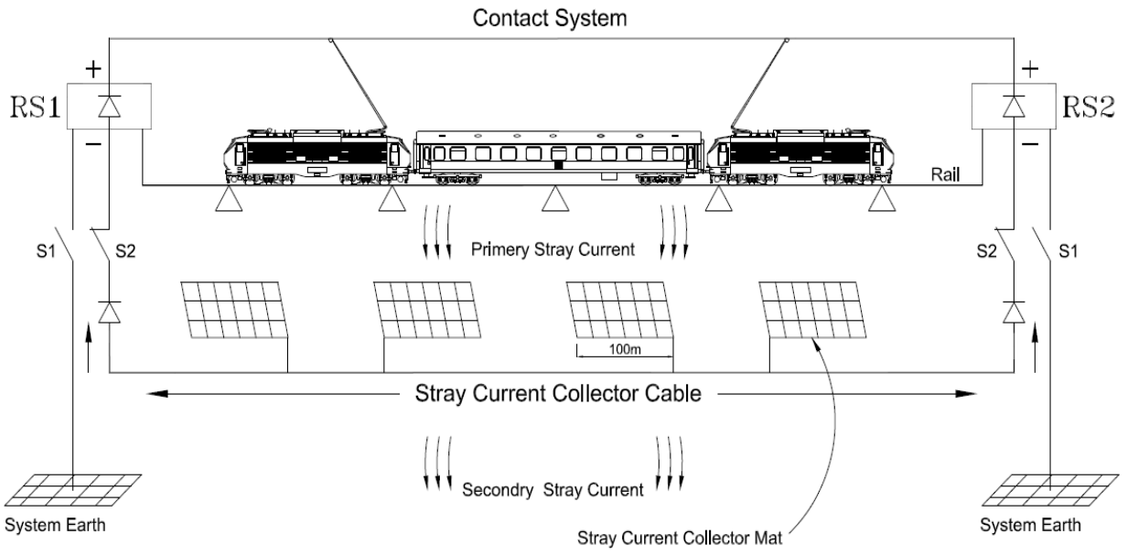


Fig. 24. Using stray current collection mat and cable

The collector cable not only creates a suitable path for the currents collected by the collection mat, but also avoids current leakage to ground due to its insulation. It directs all the collected currents to the negative substation busbar.

Fig. 25 shows the rail stray current for a line with a collector cable and when the train is at locations 100m and 300m from the initial substation. Since stray current collection mat resistance changes in comparison to resistance between rail and mat are so small, the leakage current from rail is not that much different from the previous scenario (fig.20) in floating system. But in comparison, the current captured by collection mat has increased (fig.26) and the current leakage to the ground has significantly decreased (Fig. 27). When the train is at location 300m, the total rail output current is 1.01 amperes, of which 0.049 amperes leak to the ground. In this case the efficiency of the collector system is 95%. When the train is at location 100m from the initial substation, the total rail current output is 0.33 amperes, of which 0.043 amperes enter the ground. The collector system's efficiency is 87% in this case.

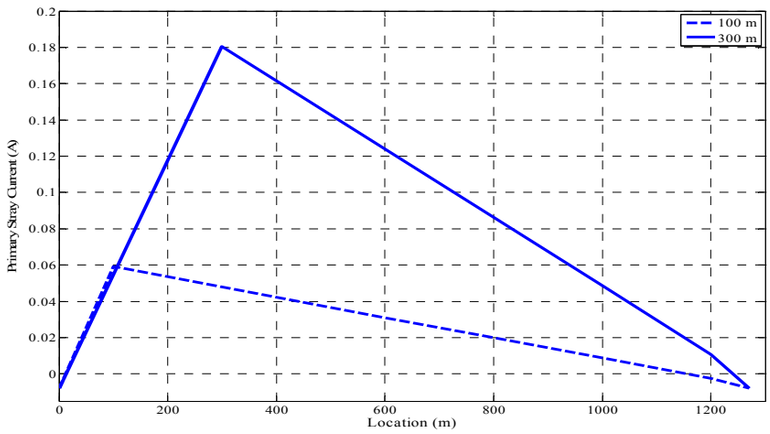


Fig. 25. The rail stray current when the train is 100 m and 300 m away from the initial substation and collector cable is used

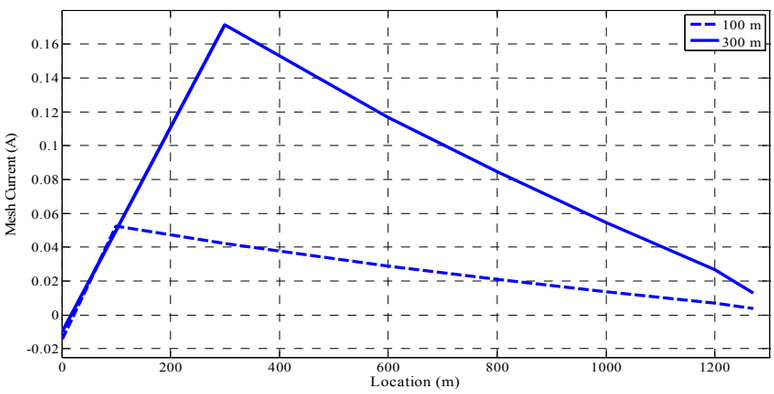


Fig. 26. The current collected by the collection system when the train is 100 m and 300 m away from the initial substation and collector cable is used

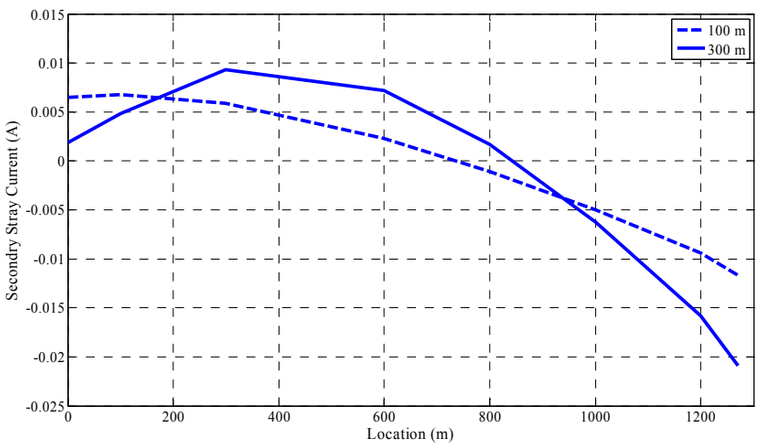


Fig. 27. Stray current leakage to ground when the train is 100 m and 300 m away from the initial substation and collector cable is used

The reason for the small effect of the collector cable on system efficiency at location 100m is the closeness of this location to the initial substation. At this short distance of the train from the substation where the rails have high current output amounts, the substation voltage cannot decrease enough so as to turn the current collector diode on. As a result, the current leakage to the ground remains high and the collector cable shows no significant effect on system efficiency. Fig. 28 shows the collector system efficiency based on the cross sectional area of the utilized cable, when the cross sectional area of mat is constant. Creation of a low resistance current path and insulation from the ground (via the collector cable) significantly decreases the stray current leakage to the ground. Changes in the cross sectional areas of the cable have effects around 1~2 % on the efficiency of the collector system. Resistances of cables with cross-sectional areas of 90 mm² and 270 mm² are 36 mΩ and 12 mΩ, respectively.

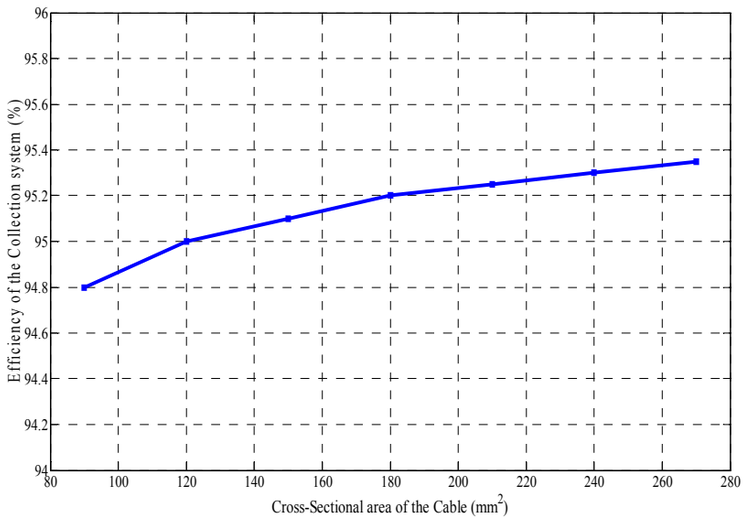


Fig. 28. Efficiency of the collector system based on the cross sectional area of the cable

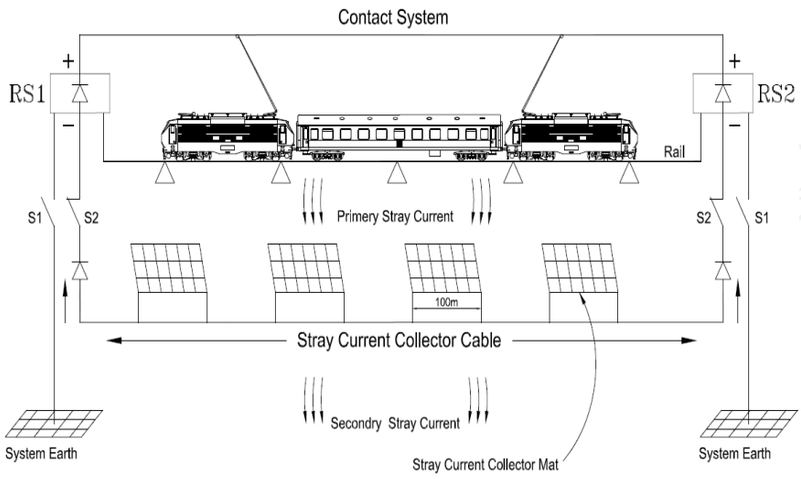


Fig. 29. Using the stray current collection mat and cable with two connection points between the mat and the cable.

The type of collector cable connections to the mats can be also changed. The above simulations were for scenarios where the mats were connected to the cables only at one point (Fig. 24). In Fig. 29, the mats are connected to the collector cables at two points. Figs 30-32 show stray current leakage from the rail, current leakage to the ground and the stray current collected by the collector system. In this case, the rail stray current becomes 1.01 amperes and the total stray current becomes 0.04, which creates an increase in system efficiency to 96.1%.

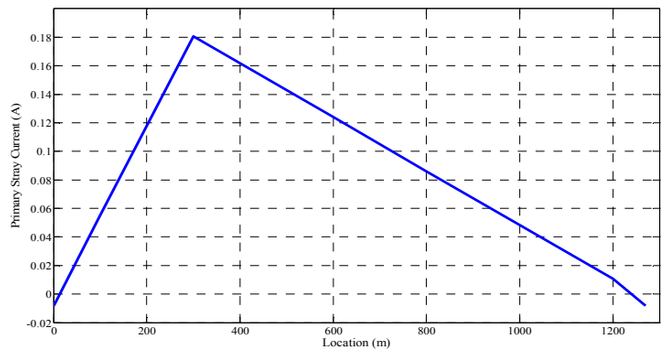


Fig. 30. The rail stray current when the train is 300 m away from the initial substation and mat and cable are connected at two points.

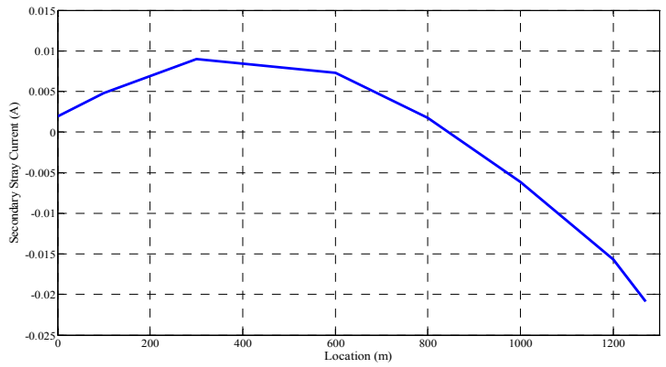


Fig. 31. Current leak to the ground when the train is at location 300 m from the first substation and the cable and mat are connected at two points.

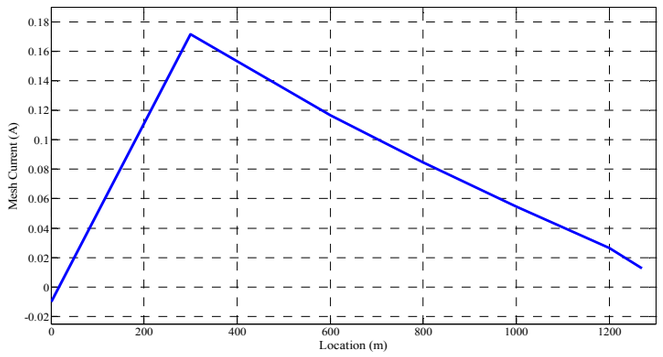


Fig. 32. The stray current collected by the mats when the train is at location 300 m from the initial substation and the cable and mat are connected at two points.

### 5.4 Simulation results in the case of usage passenger stations without traction substation

Some stations in line 4 of Tehran Metro are equipped with electrical substations. The traction power in these stations is supplied form substations of the neighboring stations. The train traction current should return to these substations via the running rails. Since the current path, compared to the previous cases, is increased, different stray current amounts and rail potentials are observed in these stations. The shorter headways between trains can result in presence of multiple trains in neighboring stations. The minimum headway in line 4 is planned to be two minutes. In this part of the research, in order to study one of the worst scenarios, the effect of presence of four trains at the following section is investigated. For this purpose, P4 station (which has no substation) and its neighboring O4 and Q4 stations (which have substation) are discussed.

In order to analyze the stray current and rail potential, four trains are assumed to be in the following locations:

Train A, in the southern line of O4 station (travel direction towards P4 station)

Train B, in the southern line of P4 station (travel direction towards Q4 station)

Train C, in the northern line of P4 station (travel direction towards O4 station)

Train D, in the northern line of O4 station (travel direction towards P4 station)

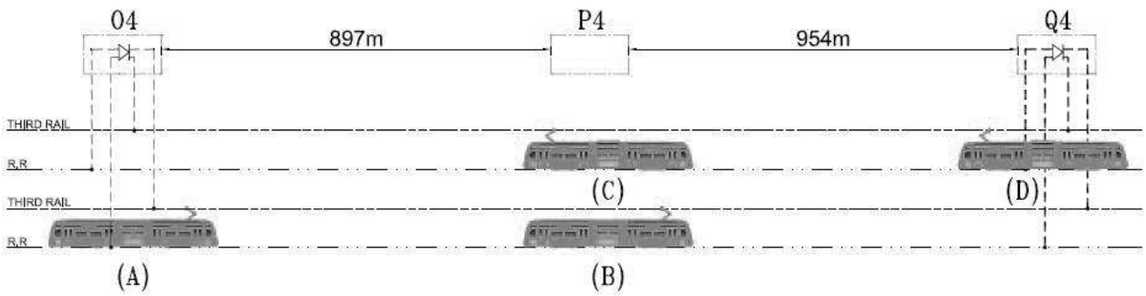


Fig. 33. Trains in the 4 train system between Q4 and O4 stations.

The order of the trains is shown in Fig. 33. It is assumed that all of the trains here start their trips simultaneously and follow the same trip profile. The mentioned parameters are investigated when the trains have traveled 300 m from their initial stations and require the highest amount of traction current. The order of trains, in this case, is shown in Fig. 34.

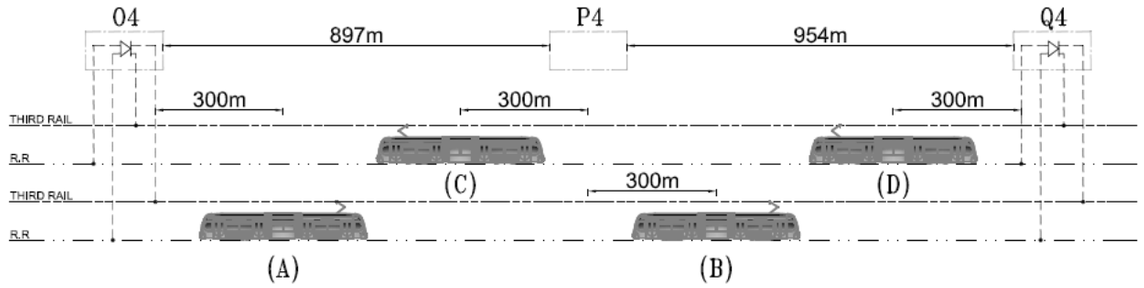


Fig. 34. Location of trains when they are 300m away from their initial stations.

Fig. 35 shows the rail stray current for the southern and northern lines when no collection mats is used. It is obvious that current leakage in P4 station is more than any other location in the line. These numbers also indicate that the rail potential is high in the neighborhood of these stations.

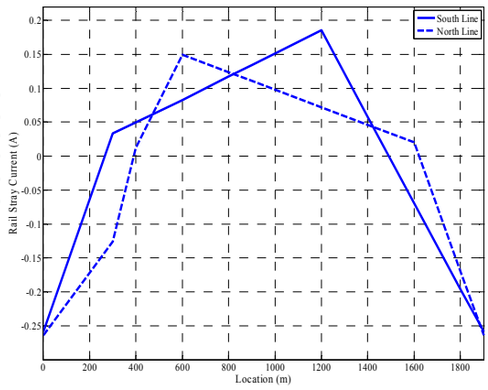


(a)

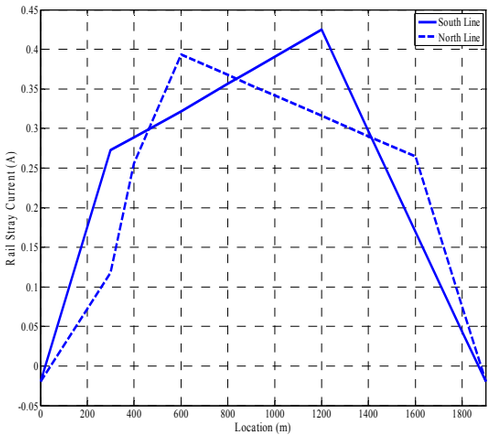


(b)

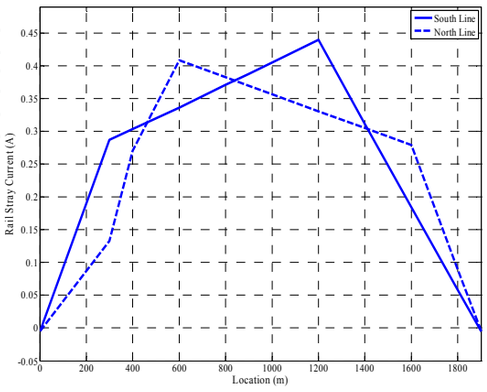


(c)

Fig. 35. The rail stray current in the four-train system in the southern and northern lines a) Floating system b) Diode grounded system c) Solidly grounded system.

The total rail stray current in the southern and northern line is 1.6 and 1.26 amperes for the floating system, 5.87 and 5.55 amperes for the diode grounded system, and 6.17 and 5.84 amperes for the solidly grounded system, respectively. These numbers are for the times when all 4 trains are consuming their maximum traction supply current from the network.

Utilizing stray current collection mats under the rails, with the previously mentioned characteristics, would highly minimize the amount of stray current leakage to the ground. Fig. 36 presents the rail voltage, rail stray current, stray current leakage to the ground and the stray current collected by the mats in the current scenario.

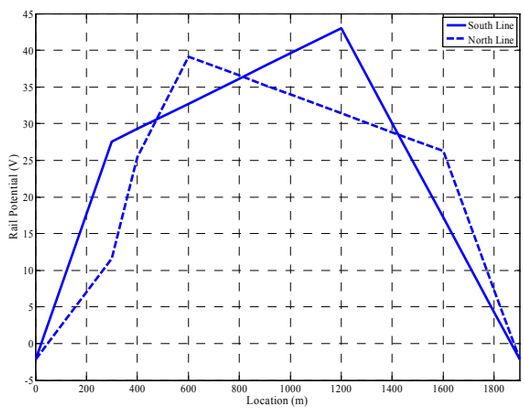


(a)

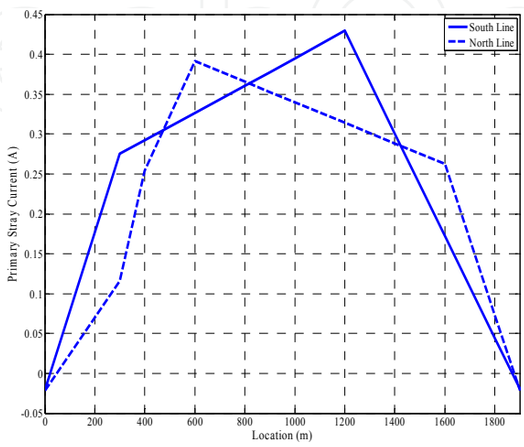


(b)

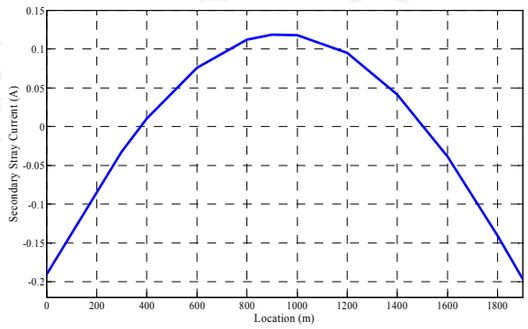


(c)

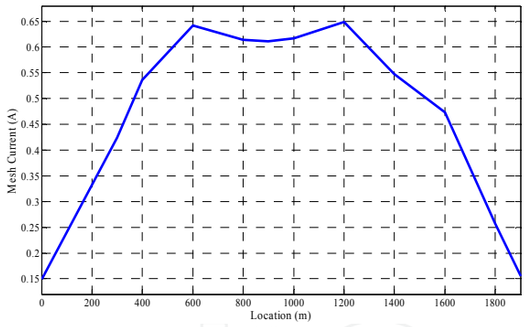


(d)

Fig. 36. The rail potential and stray current of the two lines when collection mats are used a) Rail potential b) Rail stray current c) Current leakage to the ground d) Current entering the metallic structure of the concrete.

In this case, the stray current leakage from the southern and northern lines is 5.95 and 5.51 amperes, respectively; however, only a current of 1.14 amperes leaks to the ground. In fact, the efficiency of the collector system is 90%. The system efficiency can be further improved by using a collector cable alongside the underlying collection mat, which results in even lower stray current leakage to the ground.

Fig. 37 shows the rail potential and currents in a system that has both the collection mat and the collector cable. In this system, stray current leakage from the southern and northern line is 5.96 and 5.52 amperes, respectively. Also, the current leakage to the ground is 0.71 amperes, which results in system efficiency of 94%.

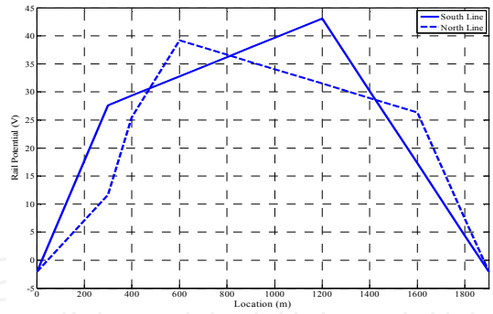


a)

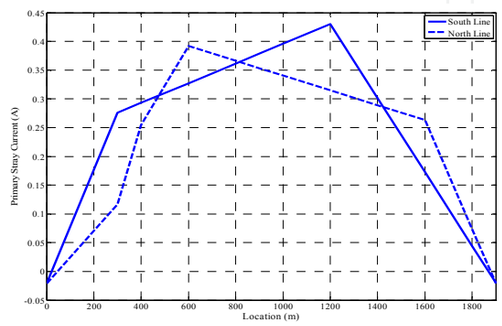


b)

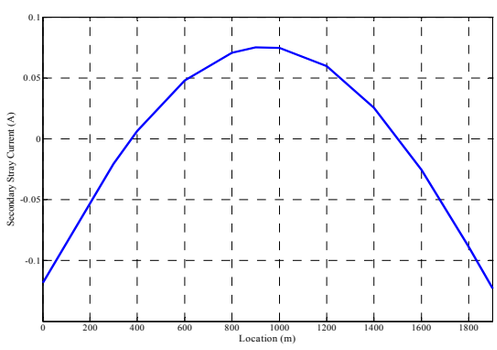


c)

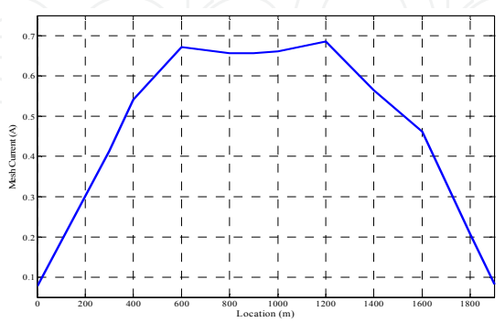


d)

Fig. 37. Rail potential and stray currents of the two lines when collection mats and collector cable are used a) Rail potential b) Rail stray current c) Current leakage to the ground d) Current entering the current collector mat.

## 6. Conclusions

Based on the performed simulations, it can be concluded that among the existing grounding schemes, the solidly grounded system creates the highest amounts of stray current. Using floating ground systems reduces the stray currents leakage. The systems that create direct rail to ground connections increase the corrosion rates significantly. The higher the connection current and the longer the time, the higher the magnitude of the resulting corrosions would be.

The metallic mats of track-beds and foundations increase the stray current leakage to the ground. The stray current travels through the mat and creates metallic corrosion in system terminations. If the mats are used as low resistance paths for absorbing stray currents and directing them to the substations, not only the corrosions of the mats, but also damages to the neighboring structures are avoided. For this purpose, the detached structures are bonded to each other and finally connected to the negative busbar of the substation. Employing stray current collection mats greatly reduces current leakages to ground. Increased cross sectional areas (of cables) and unified connectivity would further improve system efficiency and protection of the mats against corrosions. Stray current collector cables are also used for increasing system efficiency and protecting against corrosions. These cables are insulated from the ground and by collecting the stray currents from the mats, greatly diminish current leakages to soil. The cables can be connected to the collection mats at specific locations. The number of connections depends on the magnitude of stray current at a specific location.

Using collection systems as mats can help collect more than 0.85 of rails stray currents. Also addition of cables to these systems further boosts the system lifetime and stray current collection up to 0.94.

However, usage of stray current collection system causes floating system acts like diode grounded system, but as shown in the last scenario, use of voltage control device is necessary in stations without traction substations.

At locations where there is negative current leakage to the ground, the health of the existing metallic structures is threatened. Therefore it is recommended to use stray current and metallic structures voltage changes monitoring systems, at these locations, that conform to EN50122-2 standard [12].

## 7. Acknowledgements

The authors would like to thank Tehran Urban and Suburban Railway Company for assistance to perform the testing, study and evaluation. They express their appreciations to Mr. Hamed Zafari for his effort to revise this paper in English language.

## 8. References

[1] Y. C. Liu and J. F. Chen, Control scheme for reducing rail potential and stray current in MRT systems, IEE Proc. Electr. Power Appl.,2005, vol. 152issue 3, pp 612-618.

[2] D. Paul, DC traction power system grounding, IEEE Trans. Ind. Appl., 2002, vol. 38, pp 818–824.

[3] G. Yu and C. J. Goodman, Modeling of rail potential rise and leakage current in DC rail transit systems, Presented at IEE colloquium on Stray current effects of DC railways and tramways, 1990, pp 221-226.
[4] S. Case, DC Traction Stray Current Control. So What is the Problem?, Inst. Elect. Eng. Seminar (1999).
[5] C. H. Lee, and Wang, H.M., Effects of earthing schemes on rail potential and stray current in Taipei rail transit systems, IEE Proc. Electr. Power Appl., vol. 148(2001), 148–154.
[6] C. H. Lee and C. J. Lu, Assessment of Grounding Schemes on Rail Potential and Stray Currents in a DC Transit System, IEEE Trans. on Power Delivery,2006, vol. 21, pp.1941-1947
[7] C. Charalambous and I. Cotton, Influence of soil structures on corrosion performance of floating-DC transit systems, IET Electr. Power Appl., 2007, vol. 1, pp .9-16
[8] I. Cotton, P. Aylott and P. Ernst, Stray Current Control in DC Mass Transit Systems, IEEE Transaction on vehicular technology,2005, vol. 54, no.2. pp 722-730
[9] C. Lee, Evaluation of the Maximum Potential Rise in Taipei Rail Transit Systems, IEEE Transactions on Power Delivery, 2005, vol. 20, no. 2, pp. 1379-1384.
[10] C. H. Lee and Y. S. Tzeng, Assessment of grounding, bonding, and insulation on rail potential and stray currents in a direct current transit system, JRRT206, 2009, vol. 223, pp. 229-240
[11] W. M. Sim, C. F. Chan, Stray current monitoring and control on Singapore MRT system, IEEE international Conf. on power system tech., Powercon (2004), pp 1898-1903.
[12] European Standard EN 50122 -2, Railway applications - Protection again leaked currents, CENELEC, Bruxelles(1999).

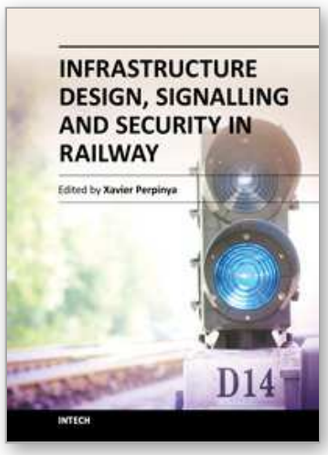


**Infrastructure Design, Signalling and Security in Railway**

Edited by Dr. Xavier Perpinya

ISBN 978-953-51-0448-3
Hard cover, 522 pages
**Publisher** InTech
**Published online** 04, April, 2012
**Published in print edition** April, 2012

Railway transportation has become one of the main technological advances of our society. Since the first railway used to carry coal from a mine in Shropshire (England, 1600), a lot of efforts have been made to improve this transportation concept. One of its milestones was the invention and development of the steam locomotive, but commercial rail travels became practical two hundred years later. From these first attempts, railway infrastructures, signalling and security have evolved and become more complex than those performed in its earlier stages. This book will provide readers a comprehensive technical guide, covering these topics and presenting a brief overview of selected railway systems in the world. The objective of the book is to serve as a valuable reference for students, educators, scientists, faculty members, researchers, and engineers.



**InTech Europe**
University Campus STeP Ri
Slavka Krautzeka 83/A
51000 Rijeka, Croatia
Phone: +385 (51) 770 447
Fax: +385 (51) 686 166
www.intechopen.com

**InTech China**
Unit 405, Office Block, Hotel Equatorial Shanghai
No.65, Yan An Road (West), Shanghai, 200040, China
中国上海市延安西路65号上海国际贵都大饭店办公楼405单元
Phone: +86-21-62489820
Fax: +86-21-62489821

IntechOpen